[CANCER RESEARCH 58, 3401–3408, August 1, 1998]

The Murine *Fhit* Locus: Isolation, Characterization, and Expression in Normal and Tumor Cells[1]

Yuri Pekarsky,[2] Teresa Druck,[2] Maria Grazia Cotticelli, Masataka Ohta,[3] Jiang Shou, Jeannine Mendrola, Jeffry C. Montgomery, Arthur M. Buchberg, Linda D. Siracusa, Giacomo Manenti, Louise Y. Y. Fong, Tommaso A. Dragani, Carlo M. Croce, and Kay Huebner[4]

Kimmel Cancer Institute, Jefferson Medical College, Philadelphia, Pennsylvania 19107 [Y. P., T. D., M. G. C., M. O., J. S., J. M., J. C. M., A. M. B., L. D. S., L. Y. Y. F., C. M. C., K. H.]; and Istituto Nazionale Tumori, Milan, Italy 20133 [G. M., T. A. D.]

ABSTRACT

The murine *Fhit* locus maps near the centromere *v* proximal *Ptprg* locus on mouse chromosome 14. The cDNA sequence and structure are similar to those of the human gene, with exons 5–9 encoding the protein. The predominant mRNA in the tissues and cell lines tested was an alternatively spliced form missing exon 3. Most murine cell lines tested, including lines established from normal mouse embryos and tumors, expressed very low or undetectable levels of *Fhit* mRNA. Most normal mouse tissues expressed wild-type *Fhit* mRNA, whereas ~40% of murine lung carcinomas expressed wild-type and aberrant *Fhit* RT-PCR products that lacked various exons. Several tumorigenic mouse cell lines exhibited homozygous deletions of *Fhit* exons. We conclude that the murine *Fhit* gene, like its human counterpart, is a target of alterations involved in murine carcinogenesis.

INTRODUCTION

The human *FHIT* gene at chromosome region 3p14.2, encompassing the most active constitutive chromosomal fragile site, is a candidate tumor suppressor gene for the most common forms of human cancer (1). Intragenic rearrangements within the *FHIT* locus, often resulting in independent deletions within both alleles (2, 3), have been observed in numerous cancer-derived cell lines and tumors derived from head and neck (4), esophagus (5), lung (6), stomach, colon (1), uterine cervix (7), and other organs.

The *FHIT* locus is >1 Mb in size, whereas the mRNA is 1.1 kb, encoded by 10 small exons, with exons 5–9 encoding a protein of 147 amino acids (M_r 16,800). Although the gene is specifically involved in loss of heterozygosity in many, if not most human cancers, point mutations in the gene are rare (2, 8). Like the p16/*CDKN2* locus, alterations occur more frequently through rearrangement within both alleles; unlike the p16/*CDKN2* locus, which is included in a single cosmid, the *FHIT* gene is very large. Even when both alleles sustain a deletion, the deletions need not overlap, making such deletions very difficult to detect in primary tumors. We and others have, thus, used RT[5] of tumor RNA followed by PCR amplification of nearly full-length products to assess *FHIT* expression in cancer cells. A large fraction of several tumor types exhibited aberrant-sized RT-PCR products that correlated with DNA and/or Fhit protein alterations (2). Some investigators have reported amplification of aberrant-sized products even from normal cell RNA (9, 10). Additionally, in many cancer cell lines and primary tumors, both normal and aberrant amplification products have been observed. Because the alterations to the *FHIT* locus in many cancer cells appeared not to fit the classic tumor suppressor paradigm, a number of investigators have suggested that the *FHIT* gene may not be a tumor suppressor gene. Alternative explanations for the very high frequency of alterations within the *FHIT* locus are: (*a*) the position of the *FRA3B* fragile region within *FHIT* leads to frequent deletion within the region, which sometimes accidentally includes *FHIT* exons; or (*b*) there is another suppressor gene(s) within the region that is the real target of the frequent loss of heterozygosity and deletion. Replacement and reexpression of Fhit in cancer cell lines lacking endogenous Fhit eliminated tumorigenicity of the lung, stomach, and kidney cancer cell lines tested, a result consistent with a role for Fhit as a tumor suppressor (11). Otterson *et al.* (12) have replaced Fhit in HeLa cells and have observed growth of a transfected clone as a tumor; however, immunohistochemistry of the HeLa tumor appears to show loss of Fhit expression in most of the tumor section. Most recently, immunohistochemical analysis of human cervical, lung, and kidney tumors using anti-Fhit antisera has shown that most of the tumors either do not express Fhit or express reduced levels of Fhit, whereas the normal epithelial counterpart cells strongly stain for Fhit (7, 13, 14). The fragile region, *FRA3B*, is highly susceptible to carcinogen damage (15, 16), which may be the case for other common fragile regions as well. A long-standing hypothesis (17) suggests that genes altered by fragile site rearrangement may be involved in cancer development and progression. The *FHIT* gene within *FRA3B* is such an altered gene. It is, thus, important, as suggested in a commentary summarizing recent studies of the human *FHIT* locus (18), to continue examination of its bonafides as a tumor suppressor and its function in normal and tumor cells. We have begun a study of the murine *Fhit* gene and its organization and expression in normal and tumor cells, with a view toward use of the murine model system to study the interactions among carcinogens, *Fhit* alterations, and tumor development.

MATERIALS AND METHODS

cDNA and Genomic Library Screening and Sequencing. One million plaques each of the mouse kidney cDNA library (Clontech, Palo Alto, CA) and mouse genomic library (bacteriophage library from strain SVJ129; Stratagene, La Jolla, CA) were screened with a human *FHIT* cDNA probe (1). Clones were purified, and DNA was isolated using standard procedures (19). Sequencing was performed using Perkin-Elmer thermal cyclers and an Applied Biosystems model 377 automated DNA sequencer. Murine *Fhit* sequences compiled during this study have been deposited in the GenBank database (accession nos. AF047699–AF047702).

Interspecific Backcross Mapping. Progeny from a (AEJ/Gn-*a* bp^H/a bp^H × *Mus spretus*)F_1 × AEJ/Gn-*a* bp^H/a bp^H backcross (20) were typed by Southern blot analysis of genomic DNA with a mouse *Fhit* cDNA probe representing exons 4–10. This probe detected common *Dra*I fragments of 3.0, 1.9, and 0.9 kb in DNA from AEJ and *M. spretus* mice and unique fragments of 8.6, 7.0, and 2.8 kb in AEJ DNA and of 6.1 and 3.3 kb in *M. spretus* DNA. The cosegregating 6.1- and 3.3-kb *M. spretus* fragments were followed in N_2 offspring of the backcross. Mapping of the *Ptprg*, *Plau*, and *Psp-rs1* (formerly

Received 3/19/98; accepted 5/26/98.

The costs of publication of this article were defrayed in part by the payment of page charges. This article must therefore be hereby marked *advertisement* in accordance with 18 U.S.C. Section 1734 solely to indicate this fact.

[1] Supported by United States Public Health Service Grants CA21124, CA39860, and CA56336 from the National Cancer Institute and a gift from R. R. M. Carpenter III and M. K. Carpenter.

[2] The first two authors contributed equally to this work.

[3] Present address: Banyu Tsukuba Research Institute, Okubo 3, Tsukuba, 300-33 Japan.

[4] To whom requests for reprints should be addressed, at Kimmel Cancer Institute, Thomas Jefferson University, Room 1008 BLSB, 233 South 10th Street, Philadelphia, PA 19107. Phone: (215) 503-4656; Fax: (215) 923-4498; E-mail: huebner@lac.jci.tju.edu.

[5] The abbreviations used are: RT, reverse transcription; RACE, rapid amplification of cDNA ends; YAC, yeast artificial chromosome; MCA, methylcholanthrene.

Psp-2) loci in this cross, using data generated from a subset of the mice used in this work, has been described previously (21). One hundred fifteen mice were typed at all four loci and were used for haplotype analysis; distances between adjacent markers were calculated from recombination frequencies determined from a larger number of mice typed at both loci. Linkage data were generated and analyzed with the computer program Spretus Madness: Part Deux (developed by Karl Smalley, Jim Averbach, Linda D. Siracusa, and Arthur M. Buchberg, Jefferson Medical College, Philadelphia, PA).

DNA and RNA Analysis by Southern and Northern Blot Hybridization. A mouse multiple tissue Northern blot (Clontech) was hybridized with a mouse *Fhit* cDNA probe using the supplier's protocol and washed at 60°C in 0.1% SDS and 0.1× SSC. For cell lines, total RNA was isolated from 1–5 × 10^8 cells using TRIZOL reagent (Life Technologies, Inc., Gaithersburg, MD). Poly(A)+ RNA was isolated from 0.2–1.0 mg of total RNA using the Mini-Oligo (dT) Cellulose Spin Column Kit (5 Prime-3 Prime). Three μg of poly(A)+ RNA from each cell line were electrophoresed in 0.8% agarose gel in a borate buffer containing formaldehyde and transferred to HybondN+ (Amersham, Arlington Heights, IL). For RT-PCR analysis of mouse lung tissue and tumors, total RNAs were extracted using Ultraspec-II RNA Kit (Biotecx, Houston, TX) according to previously described methods (22, 23). Restriction enzyme digestions, transfers to membrane, and hybridizations were performed as described previously (21).

PCR and RT-PCR Amplification. PCR amplification of *Fhit* exons from cellular DNA templates was performed essentially as described (2) using murine *Fhit* specific primers. Nested RT-PCR amplification of *Fhit* from murine total RNAs was performed as described for the human gene (2) or by the following modified method. Two hundred ng of poly(A)+ RNA or 3 μg of total RNA were treated with DNaseI (amplification grade; Life Technologies, Inc.) following the manufacturer's protocol. DNase-treated RNA was used in RT reactions as follows: 10 nM each dNTP, 100 pmol of random hexamers [oligo(dT) priming was used in some cases], DNase I-treated RNA, and 200 units of MuLV reverse transcriptase (Life Technologies, Inc.), in a total volume of 20 μl, were incubated at 42°C for 1 h; then 10 μg of RNase A were added, followed by incubation at 37°C for 30 min. One μl of the reaction or 100 ng of genomic DNA were used for each PCR. PCR primers and their locations are shown in Table 1. PCRs were carried out under standard conditions using 10 pmol of each gene-specific primer and 25–35 cycles of 95°C for 30 s, 55–60°C for 30 s, and 72°C for 1 min. In some cases, nested PCR was performed using 0.1 μl of the original PCR. Products were separated on 1.5% agarose gels and sometimes isolated and sequenced or cloned and sequenced.

F9 and ES RT-PCR products were ligated into the pCR2.1 vector (Invitrogen, San Diego, CA) using the procedure recommended in the TA Cloning Kit, and 1 μl of the ligation reaction transformed into DH5α-competent cells. Several colonies were selected, and plasmid DNA was isolated (Qiagen) for sequencing.

Cell Lines. Murine cell lines were purchased from American Type Culture Collection (WEHI164, CRL1412, LMTK$^-$, L929, and A9) or obtained from other investigators at the Kimmel Cancer Institute (ES, NP3, RENCA, Cl1D, MEL, IT22, BW5147, and F9). The murine melanoma cell lines K1735cl10, K1735cl4, and K1735M2X21 were obtained from Dr. Sen Pathak (M. D. Anderson Cancer Center; 24) and lines ME1 and ME2 were established in our laboratory from mouse embryos, by standard tissue culture procedures, and were passaged for 20 subcultures during these studies. Cell lines were maintained in MEM or RPMI supplemented with 10% fetal bovine serum. Cellular DNA was prepared from proteinase K-treated cell lysates by standard phenol/chloroform extraction and ethanol precipitation.

RACE. Oligo(dT)-primed double-stranded cDNA was synthesized using mouse kidney mRNA (Clontech) and procedures and reagents from the Marathon RACE cDNA amplification kit (Clontech); the cDNA was ligated to Marathon adapters (Clontech). 3′ and 5′ RACE products were generated by long-range PCR using gene-specific primers and the AP1 primer (Clontech). To increase the specificity of the procedure, the second PCR was carried out using nested gene-specific primers and the AP2 primer (Clontech). PCRs were performed according to the Marathon protocol using the Expand long template PCR system (Boehringer Mannheim) and 30 cycles of 94°C for 30 s, 60°C for 30 s, and 68°C for 4 min. RACE products were electrophoresed, identified by hybridization, and sequenced.

YAC Clone Isolation and Characterization. DNA pools from the WI/MIT 820 strain C57BL/6J YAC library were purchased from Research Genetics (Huntsville, AL). Pools were screened by PCR with the exon 1 primers according to the supplier's protocol. YAC DNAs were isolated in solution, and agarose plugs were prepared as described (25). Pulsed-field gel electrophoresis was carried out using the CHEF MAPPER pulsed-field electrophoresis system (Bio-Rad, Richmond, CA) with a pulse time of 60 s for 15 h, followed by 90 s for 9 h. DNA from gels was transferred onto a nylon membrane and hybridized with mouse *Fhit* cDNA under standard conditions.

Immunohistochemical Methods. Routine deparaffinization from xylene through a graded alcohol series and rehydration, prior to microwave antigen recovery, were carried out on a Leica Autostainer (Leica, Inc., Deerfield, IL). The deparaffinization process included a 30-min hydrogen peroxide block for endogenous peroxidase activity. The antigen recovery step was carried out in an 800-W microwave oven in 200 ml of ChemMate H.I.E.R. Buffer, pH 5.5–5.7 (Ventana Medical Systems, Tucson, AZ).

The slides were cooled and washed in distilled H_2O and placed in ChemMate Buffer 1 (PBS containing carrier protein and sodium azide). The immunostaining was performed on a Techmate 1000 (Ventana Medical Systems, Tucson, AZ) using capillary gap technology. Tissue sections were exposed for 10 min to 10% normal goat serum, followed by overnight primary antibody incubation (1:600). The primary antibody was a commercially prepared polyclonal chicken immunoglobulin raised against purified human Fhit protein. The next day, slides were washed, incubated for 30 min with a biotinylated goat antichicken IgY secondary antibody (1:200), and exposed to avidin-biotin complex for 45 min. Following a wash, slides were subjected to a 10-min application of 3,3′-diaminobenzidine. Slides were also lightly counterstained with hematoxylin and coverslipped using Permount (Fisher) mounting medium prior to evaluation.

To assess specificity of staining, ~1.5 μg/ml purified gstFhit protein was added during the overnight incubation of the tissue with antiserum.

Western Blot Analysis. Mouse cell lines and tissues were lysed, and total protein was prepared as described previously (2). Approximately 75 μg of total protein were electrophoresed on a 14% SDS-polyacrylamide gel. The membrane was prepared and blocked as described previously (2) before incubation for ~17 h at 4°C with chicken anti-Fhit (1:2000). After three 10-min washes, in TBST buffer, the blot was incubated for 1 h with rabbit antichicken IgG heavy and light chain horseradish peroxidase-labeled antibody (Pierce, Rock-

Table 1 *Oligonucleotide primers for PCR amplication*

Numbers in primer names refer to the cDNA nucleotide sequence number for the first nucleotide of the primer; primers in capital letters are within exons, and those in lowercase letters are in introns. Primer pairs spanning several exons were used in amplification from reverse transcripts; primer pairs within or flanking individual exons were used in detection of homozygous deletion of exons in cellular DNAs.

Primer pair	Sequence (5′ → 3′)	Location	Product size (bp)
MF105F/MF826R	TTTGAAGCCCAGCAAAGAAGGGA/GCCTTGGGAATCGTTTGAGTTAC	Exon 2/10	722
MF127F/MF806R	AATCCACTGTGAAGAGTCAGGAA/TACTCTCAGGCCTGAAAGTAGAC	Exon 2/10	680
MF68F/MF843R	CTTGCCTTTCATTCCAGC/GGGGTCCATTTTCTTAT	Exon 1/10	776
MF106F/MF792R	TGAAGCCCAGCAAAGAAG/AAAGTAGACCCGCAGAGC	Exon 2/9	687
MF1F/MF77R	GTCAGTTCCCAGGTCCAC/ATCTTGGTGGCTGGAATG	Exon 1	77
MF170F/MF261R	TACTTTGGAATACCTCCTCACAG/CTTCAGATTAGTCCAACCTATCAG	Exon 3	92
mfiex5F/R	GAGGGACAATTAAAAGGGAC/ATTCCTTGCTTACCTTTTGG	Intron 4/intron 5	361
mfiex6F/R	CCCTCAAAGTAAACCAACAA/AAATGCAGACCACAAAAACC	Intron 5/intron 6	456
mfiex7F/MF623R	GGCCTGCTGGATAATTCATA/ACAGTCTGCCCAGCTTCA	Intron 6/exon 7	260
mfiex8FMF696R	CACTGTCAAGTCAAAATATAG/CTCATCATAGATGTTGTCATT	Intron 7/exon 8	135

ford, IL) diluted 1:40,000. Signal was detected using the Super Signal chemiluminescent substrate (Pierce).

Mouse Lung Tumors. Male and female A/J, C3H/He, and BALB/cJ mice were purchased from The Jackson Laboratory (Bar Harbor, ME) and then crossed in our laboratory (26). Lung tumors were induced by a single i.p. injection of 300 mg of urethane dissolved in water per kg body weight (27). The tumors were excised from female mice and ranged from 4 to 15 mm in diameter. Normal lungs were excised from untreated adult (A/J × C3H/He)F_1 female mice.

RESULTS

***Fhit* cDNA Sequence and Genomic Structure.** The mouse kidney cDNA library was screened using the human *FHIT* cDNA; after tertiary screening, the few positive cDNA clones were amplified, sequenced, and compared to human *FHIT* cDNA sequence and to the public databases. The first cDNA clone was found to represent exons 4–10. The 5′ sequence was determined by performing 5′ RACE on a reverse transcript of mouse kidney RNA. Primer pairs from different regions of the murine *Fhit* cDNA were used to amplify different overlapping fragments of the cDNA reverse-transcribed from RNA derived from a number of tissues and cell lines. PCR-amplified fragments were also sequenced so that each portion of *Fhit* cDNA was sequenced numerous times to assemble the full sequence shown in Fig. 1*B*. Oligonucleotide primer pairs used in amplification of *Fhit* fragments are listed in Table 1.

Primer pairs within exon 1 were used to screen the mouse YAC library, and several YAC clones were identified. YAC clone 158E2 appeared to be part of the WC14.2 contig in the Whitehead/MIT

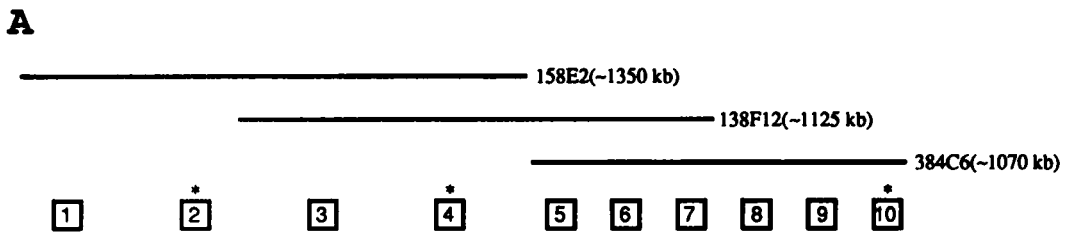

B

```
   1  GTCAGTTCCCAGGTCCACCCCAGTGGGGACACGATCAGGCGGCACTCCTGTCCTGTGCTC   60
                                                  1\/2$
  61  CCGCCCTCTTGCCTTTCATTCCAGCCACCAAGATCTTGGCAGCTTTGAAGCCCAGCAAAG  120
                                        2\/3
 121  AAGGGAAATCCACTGAGAAGAGTCAGGAAAGGCACATGAATGCTCAGCCTACTTTGGAAT  180
                                           *** M  L  S  L  L  W  N

 181  ACCTCCCCACAGTGCAACCAAATGCAAGACGTTGGTGCCTTCAAGATAGTATTCTACCTG  240
      T  S  P  Q  C  N  Q  M  Q  D  V  G  A  F  K  I  V  F  Y  L
                        3\/4
 241  ATAGGTTGGACTAATCTGAAGGTGCCCTGGGACAACCTGCTCGGTCACACATCTGCAAGA  300
      I  G  W  T  N  L  K  V  P  W  D  N  L  L  G  H  T  S  A  R
                              4\/5
 301  ACTCTCCATCTTGCACTGAGGACCCCAAGGAGCTTTTACTGTGAGACCATGTCATTTAGA  360
      T  L  H  L  A  L  R  T  P  R  S  F  Y  C  E  T  M  S  F  R    4

 361  TTTGGCCAACATCTCATCAAGCCCTCTGTGGTTTTTCTCAAAACTGAACTGTCCTTCGCC  420
      F  G  Q  H  L  I  K  P  S  V  V  F  L  K  T  E  L  S  F  A   24
                                    5\/6
 421  CTGGTGAATAGGAAACCCGTTGTACCTGGCCATGTCCTCGTGTGCCCGCTGAGGCCAGTA  480
      L  V  N  R  K  P  V  V  P  G  H  V  L  V  C  P  L  R  P  V   44

 481  GAGCGCTTCCGTGACCTACATCCTGATGAAGTGGCCGATTTGTTTCAAGTGACCCAGAGA  540
      E  R  F  R  D  L  H  P  D  E  V  A  D  L  F  Q  V  T  Q  R   64
               H        R                                T      6\/7
 541  GTTGGGACAGTGGTGGAGAAGCATTTCCAGGGGACCTCCATCACCTTCTCCATGCAAGAT  600
      V  G  T  V  V  E  K  H  F  Q  G  T  S  I  T  F  S  M  Q  D   84
                              H
                           7\/8
 601  GGTCCTGAAGCTGGGCAGACTGTGAAGCATGTACATGTCCACGTTCTTCCCAGGAAGGCA  660
      G  P  E  A  G  Q  T  V  K  H  V  H  V  H  V  L  P  R  K  A  104
                                          8\/9
 661  GGGGACTTCCCCCGGAATGACAACATCTATGATGAGCTCCAGAAACATGACAGAGAAGAA  720
      G  D  F  P  R  N  D  N  I  Y  D  E  L  Q  K  H  D  R  E  E  124
               H           S        E                 K
 721  GAGGACTCGCCAGCCTTTTGGAGATCTGAGAAGGAGATGGCTGCAGAGGCGGAGGCTCTG  780
      E  D  S  P  A  F  W  R  S  E  K  E  M  A  A  E  A  E  A  L  144
            F        S        9\/10$              A
 781  CGGGTCTACTTTCAGGCCTGAGAGTAACTCAAACGATTCCCAAGGCATAAGAAAATGGAC  840
      R  V  Y  F  Q  A  ***                                       150

 841  CCCATTCTTCTGGAGTCTTCGACATTGGAAATGAAGCTAACCACTCTTTATTGTACCCCA  900
 901  CGACCCCACAGCCTTGTACAAAGAACTTTATTGCATGTGTGGAAGCCACTAGTATTATGC  960
 961  TTCCATCACGATGACAAATAGGCTAGCTTCCCAAACAGTGGCATTGACAGCCTGCCACCG 1020
1021  TTCCTCAGTTCTGTACTTAGAATANTAACATTTCCAAACTGTCCCTGAACCTAGATGAAA 1080
1081  ATAAAGTTGGTTGCT
```

Fig. 1. Genomic structure and cDNA sequence of the mouse *Fhit* gene. *A*, YAC contig covering the gene. The mouse *Fhit* gene is 1.2–2 Mb in size. YAC names and sizes are indicated. *, provisional exon positions. *B*, mouse *Fhit* cDNA. Exon boundaries are shown above the sequence. $, provisional exon boundaries based only on homology between human and mouse cDNAs. *Underlined letters*, amino acid sequence encoded by the major transcript (that lacks exon 3). Amino acids that differ in human Fhit protein sequence are shown below the murine amino acid sequence. *Boldface letters*, amino acids that are absent in human protein.

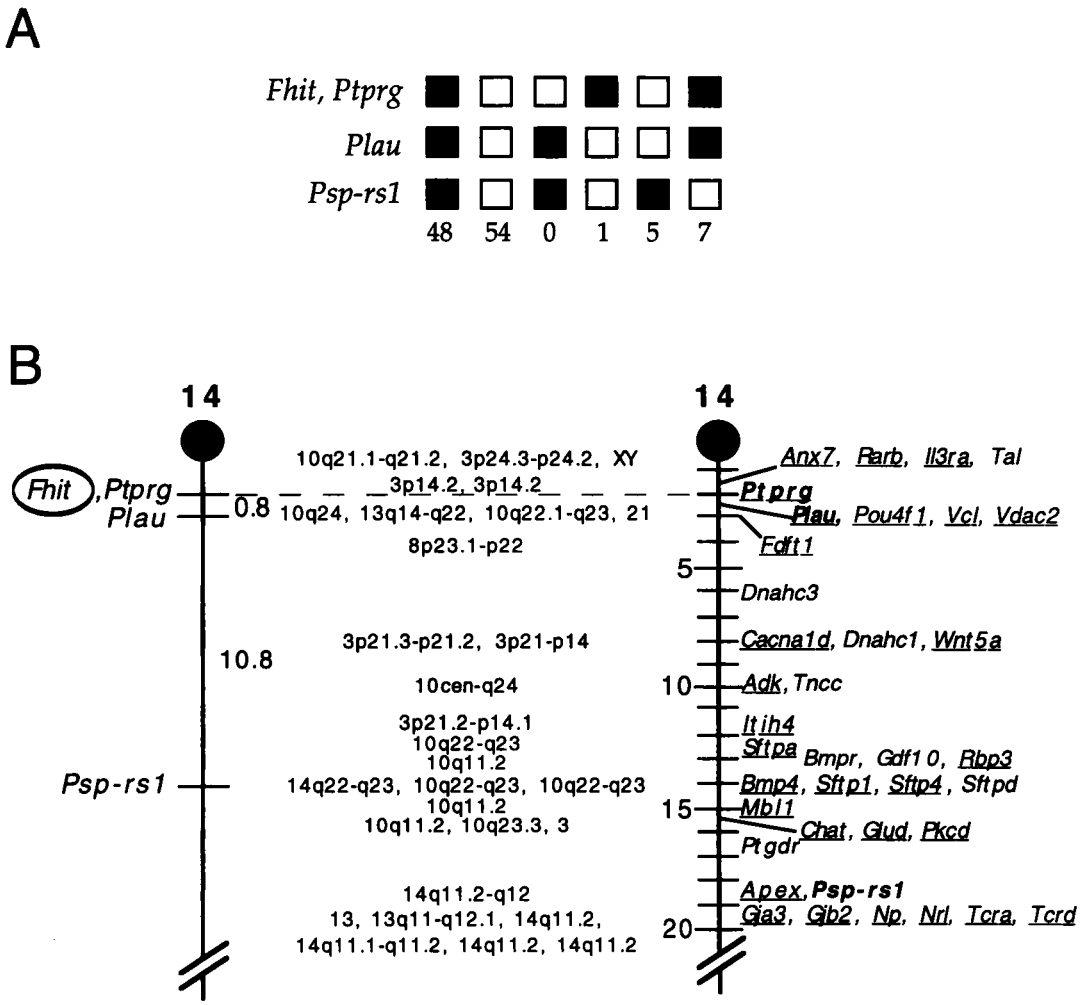

Fig. 2. Chromosomal location of mouse *Fhit*. *A*, haplotype analysis of 115 N_2 offspring from the interspecific backcross. *Left*, mapped loci. Each column represents the chromosome inherited from the (AEJ/Gn × *M. spretus*)F_1 parent. ■, AEJ/Gn alleles; □, *M. spretus* alleles. *Numbers*, number of progeny carrying that particular haplotype. *B*, genetic linkage map showing the position of *Fhit* in the mouse genome. *Left*, chromosome showing the loci typed in the interspecific backcross with intergenic distances given in cM. *Right*, chromosome that is a partial representation of the chromosome 14 committee report consensus map (accessible on-line via the Mouse Genome Database at www.informatics.jax.org). Distances from the centromere are given in cM. - - - - -, locus used to align the maps. *Underlined loci*, loci that have been mapped in the human genome; their gene locations on human chromosomes are shown between the maps.

database. YACs 138F12 and 384C6 from this contig appeared to cover the entire *Fhit* locus (Fig. 1*A*), as determined by PCR amplification and Southern hybridization. Sizes of the YACs were determined by pulsed-field gel electrophoresis of DNA from each of the YACs; the assembled contig (Fig. 1*A*) suggests that the mouse *Fhit* locus is, like the human, 1–2 Mb in size. DNA from the YACs was also digested with enzymes that do not cleave within *Fhit*, and Southern blot hybridizations were performed to determine the presence and size of individual *Fhit* exons within the YACs.

The murine *Fhit* protein is 91% identical to human and 93% similar; the amino acids that differ are indicated in Fig. 1*B*. This figure also shows that upstream of the exon 5 Met codon, which is the putative start codon for the Fhit protein (Fig. 1*B*, *underlined letters*), there is a conceptual open reading frame extending into exon 3. This start codon would rarely be used, however, because the main murine *Fhit* transcript is an alternative transcript with exon 2 spliced to exon 4, eliminating exon 3 and its Met codon (see below). The ~11-kb exon 5 genomic fragment is 38% GC, the ~15-kb exon 6 genomic clone is 38.7% GC, and the ~2-kb exon 8 genomic fragment is 38.1% GC, suggesting that the mouse *Fhit* locus, like the human (3), may have an overall high AT content.

The *Fhit* cDNA probe was used in linkage analysis to determine the chromosomal location of the murine gene. Interspecific backcross analysis of 115 N_2 mice showed that the *Fhit* locus cosegregated with several previously mapped loci from the centromere proximal end of chromosome 14. The distribution of haplotypes shown in Fig. 2 indicates the following gene order: centromere-*Ptprg*-*Fhit*-(0.8 ± 0.8 cM)-*Plau*-(10.8 ± 2.8 cM)-*Psp-rs1*-telomere. No recombination between the *Fhit* and *Ptprg* loci in 187 N_2 animals suggests tight linkage, with a maximum distance between the two genes of 1.6 cM (95% confidence).

The cDNA probe was also used in selection of *Fhit* genomic clones from the 129/SvJ library; clones for exons 5, 6, and 8 were obtained, and intron-exon boundaries were sequenced, as described previously (2, 28). A ~8-kb PCR product containing intron 6 was amplified from mouse YACs 138F12 and 384C6, purified, and sequenced. Other exon boundaries were determined by sequencing of alternative transcripts (see below). Primer pairs flanking exons 5, 6, 7, and 8 were then designed (see Table 1) to test DNAs from murine cell lines for presence of these exons. Primer pairs within exons 1 and 3 (Table 1) were designed and used in similar experiments. Results are summarized in Table 2, and examples of the homozygous deletions detected are shown in Fig. 3, which illustrates the absence of exon 5 in the BALB/c derived renal carcinoma cell line RENCA (see Fig. 3*A*, *Lane*

Table 2 *The Fhit locus in murine cell lines*

Cell line	Origin	*Fhit* exons	Fhit RT-PCR	Northern blot
ES	Embryonic stem	+[a]	Wild type[b]	
F9	Teratocarcinoma	+	Wild type	
ME1	Mouse embryo	+	Wild type	+[c]
ME2	Mouse embryo	+	Wild type	+[c]
IT22	3T3 TK$^-$ clone	+	−	−
NP3	Myeloma	+		
MEL	FeLv erythroleukemia	− exons 6, 7, 8	−	
BW5147	Thymoma	+		
LMTK$^-$[d]	MCA-treated adult connective tissue	+	+ exons 5–10	+ short[e]
WEHI164	MCA-induced fibrosarcoma	+	−	−
CRL1412	C3H10t1/2 MCA-treated	+	−	−
RENCA	Kidney carcinoma	− exon 5		
K1735c110	Melanoma	+	−	−
K1735M2X21	Metastatic clone	+	−	−

[a] Presence of exons 1, 3, 5, 6, 7, and 8 was detected in genomic DNA from cell lines by PCR amplifications using intron primers flanking exons 5, 6, 7, and 8 or primers within exons 1 and 3. +, all six exons were present.

[b] Wild-type RT-PCR product consisted of three species in mouse tissues and cell lines, as described in Fig. 3 legend.

[c] ME1 and ME2 showed a very faint signal of expected size on Northerns.

[d] LMTK$^-$, a clone of L cells, was previously shown to be missing exons 3–5 of the *Ptpγ* gene, as were all L-derived lines tested (21).

[e] LMTK$^-$ Fhit mRNA was abundant but shorter than the expected size (see Fig. 2) and had an aberrant 5′ untranslated region.

5), and the absence of exon 6 in the Feline leukemia virus-induced murine erythroleukemia cell line, MEL (Fig. 3*A*, *Lane 12*). The MEL cells also lack exons 7 and 8 (data not shown). Other cell line DNAs exhibited presence of each of the exons tested, as summarized in Table 2. Exons 2, 4, and 9 are too small to detect using primer pairs within them. Some cellular DNAs were also tested for integrity of the *Fhit* locus by Southern blot analysis, and alterations in additional cells were not detected. Restriction fragment length polymorphisms were observed for exon 3 (*Xba*I, 3.7 or 3.3 kb) and exon 8 (*Bam*HI, 18 or 6.7 kb; *Xba*I, 5.8 or 2.6 kb). Fig. 3*B* illustrates the *Xba*I polymorphism of exon 8, as well as the absence of exons 6 and 7 in MEL cells (Fig. 3*B*, *Lane 1*;, note that absence of exon 8 is obscured by overlap of the exon 4 fragment with the position of exon 8 allele *a1*). Homozygous deletion of exon 5 in RENCA cells is also confirmed by the Southern blot results (Fig. 3*B*, *Lane 2*).

***Fhit* Transcription.** To identify murine tissues that express the *Fhit* gene, a commercially prepared Northern blot that contained 2 μg per lane of poly(A)$^+$ RNA from eight adult mouse tissues was hybridized first to a *Fhit* exon 4–10 probe and, after stripping, to a β-actin probe (Fig. 4, *A* and *B*). Each of the tissues expressed the ~1-kb *Fhit* mRNA, with liver and kidney (*Lanes 5* and *7*) displaying the most intense signals and testes and brain (*Lanes 2* and *8*) showing moderate signals. Similar Northern blot analysis of *Fhit* expression in murine cell lines is illustrated in Fig. 4*C*. Two mouse embryo-derived cell lines (*Lanes 2* and *3*) produce barely detectable *Fhit* mRNA (signal was barely visible on X-ray after several days of exposure). Two melanoma-derived clones do not express detectable *Fhit* mRNA (*Lanes 4* and *5*). The CRL1412 cell line (*Lane 6*) was a C3H 10t1/2 mouse embryo-derived cell line treated with MCA; the cells reportedly produce fibrosarcomas on inoculation into syngeneic mice and are negative for *Fhit* expression. *Fhit*-negative WEHI164 cells (*Lane 7*) were established from a fibrosarcoma induced by MCA injection in a BALB/c mouse. LMTK$^-$ (*Lane 8*) is a tumorigenic clonal derivative of the original L strain derived from s.c. tissue of an adult male mouse established in culture with *in vitro* MCA treatment. The cell line produces sarcomas in nude mice. As shown in Fig. 4*C*, *Lane 8*, LMTK$^-$ cells express a shortened *Fhit* transcript. IT22 cells, a clonal derivative of Swiss 3T3 cells, are negative for expression of *Fhit* exons 5–10 (Fig. 4C, *Lane 9*) but express a range of aberrantly sized mRNAs detected by exons 1–4 (data not shown). Fig. 4*D* shows the ethidium bromide-stained gel for the Northern blot in Fig. 4*C*; rehybridization of the blot to a β-actin probe showed equal amounts of signal in all lanes (data not shown).

RNAs from a larger panel of mouse cell lines were examined for expression of *Fhit* by RT-PCR amplification. These studies were carried out using various protocols: unnested amplification of exons 2–9; nested amplification with outer primers in exons 1 and 10, followed by amplification using primers in exons 2 and 9; and single-round amplification of exons 1–4, 5–9, or 10 and other combinations. Consistent amplification of expected products was obtained from RNA of ES cells, F9, F9 differentiated, ME1, and ME2 cell lines and all murine tissues tested. The expected size exon 5–10 product was amplified from LMTK$^-$ RNA, although a product representing the 5′ untranslated region (exons 1–4) was not detected. Sequencing of LMTK$^-$ 5′ RACE product revealed that LMTK$^-$ *Fhit* mRNA

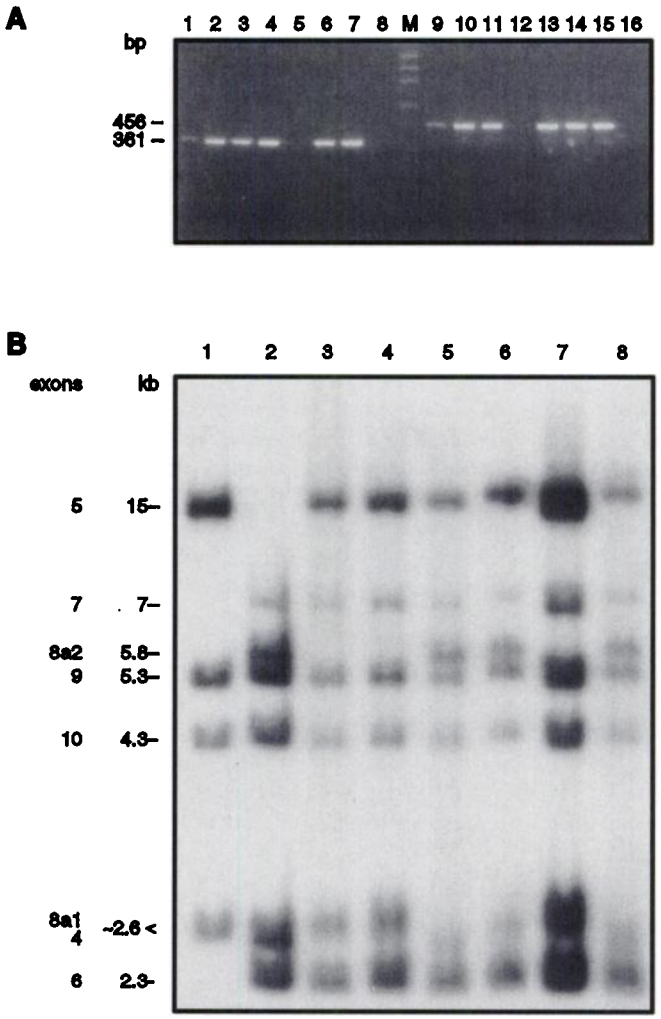

Fig. 3. Presence of *Fhit* exons in murine cell lines. *A*, template DNA (100 ng) was amplified by PCR using primer pairs flanking exon 5 (*Lanes 1–8*) or primer pairs flanking exon 6 (*Lanes 9–16*). DNAs were from mouse cell lines: A9, an L cell clone (*Lanes 1* and *9*), K1735 primary (*Lanes 2* and *10*), K1735M2X21 (*Lanes 3* and 11), MEL (*Lanes 4* and *12*), RENCA (*Lanes 5* and *13*), WEHI164 (*Lanes 6* and *14*), and ME2 (*Lanes 7* and *15*). *Lanes 8* and *16*, negative controls for amplification without DNA template. *B*, absence of exons was also observed by Southern blot analysis of *Xba*I-digested DNAs (10 μg) of murine cell lines hybridized to a *Fhit* exon 4–10 probe: *Lane 1*, MEL; *Lane 2*, RENCA; *Lane 3*, K1735c110; *Lane 4*, K1735M2X21; *Lane 5*, WEHI164; *Lane 6*, ME1; *Lane 7*, A9 L cell clone; *Lane 8*, IT22 Swiss 3T3 clone. The sizes of specific restriction fragments are shown at the *left*, and exons contained in specific fragments are indicated. *Xba*I detects an exon 8 polymorphism of ~5.8 (*8a2* in *B*) or ~2.6 kb (*8a1* in *B*), as well as an exon 3 polymorphism (3.7 or 3.3 kb, data not shown; *B*, probe lacked exon 3).

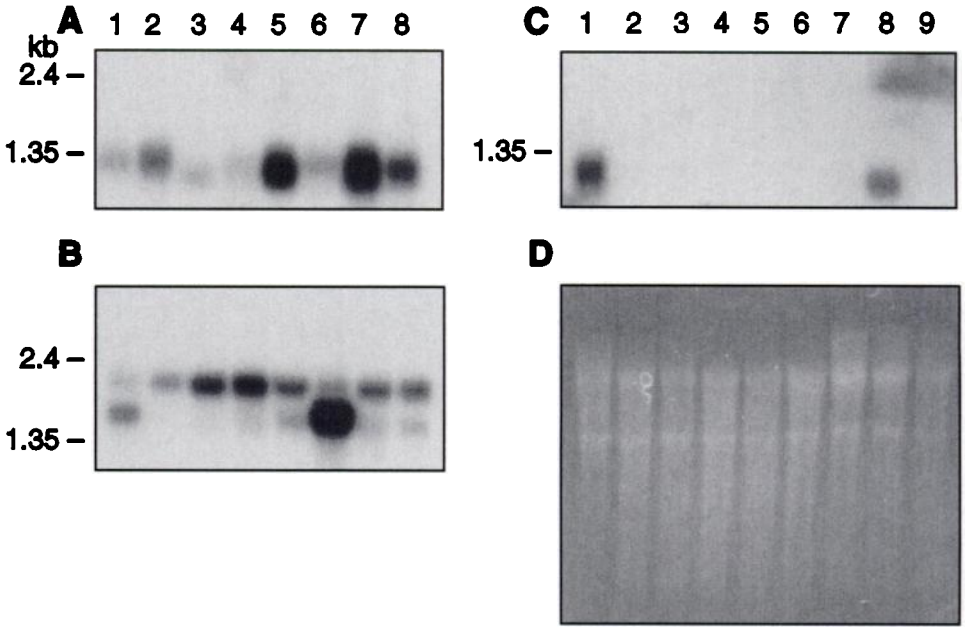

Fig. 4. Expression of *Fhit* mRNA in tissues and cell lines. Two μg of mRNA from adult murine tissues or from murine cell lines were electrophoresed, transferred to membrane, and hybridized to radiolabeled cDNA probes. *A*, mRNA from heart (*Lane 1*), brain (*Lane 2*), spleen (*Lane 3*), lung (*Lane 4*), liver (*Lane 5*), muscle (*Lane 6*), kidney (*Lane 7*), and testes (*Lane 8*) hybridized to radiolabeled *Fhit* exon 5–10 probe. *B*, the membrane shown in *A* was stripped and hybridized to radiolabeled β-actin cDNA. *C*, mRNA from mouse brain (*Lane 1*), cell lines ME1 (*Lane 2*), ME2 (*Lane 3*), K1735M2×21 (*Lane 4*), K1735c110 (*Lane 5*), CRL1412 (*Lane 6*), WEHI164 (*Lane 7*), LMTK$^-$ (*Lane 8*), and IT22 (*Lane 9*) was hybridized to radiolabeled *Fhit* exon 5–10 probe. *D*, ethidium bromide-stained gel photographed before transfer of mRNAs from the gel, illustrating quality and quantity of mRNA; the RNAs shown in *C* were transferred from this gel.

lacks exons 1–4 and exhibits an unknown 100-bp sequence 5′ of exon 5 (data not shown). Results are summarized in Table 2. Examples of the RT-PCR products amplified and analyzed are shown in Fig. 5*A*. As shown in *Lanes 4* (ME1), *8* (ME2), and *9* (mouse brain), at least three products were amplified from the freshly established mouse embryo cell lines and the mouse brain. The products were cloned and sequenced and compared to full-length *Fhit* cDNA. The most intense product, at just above the 500-bp marker, represents an alternatively spliced transcript that lacks exon 3; the larger product retains exon 3, and the smaller product lacks exons 3 and 4. The transcript lacking exon 3 was reproducibly the major transcript in all tissues and cell lines expressing *Fhit*. This transcript would lack the upstream potential starting Met codon, leaving the first Met codon in exon 5 as the likely major translation start site. The ME1 and ME2 cells showed the same products at tissue culture passages 2 and 20 without obvious differences in quality or quantity.

RNAs from 30 urethane-induced mouse lung tumors also served as templates for RT-PCR amplification. Twelve of the 30 (40%) showed shorter fragments, in addition to the expected wild-type products; examples are shown in Fig. 5*B*. *Lanes 1–9* contain RT-PCR products from nine lung tumors; aberrant products were amplified from four of these nine (*Lanes 5*, *7*, *8*, and *9*). The aberrant products from all tumors were sequenced and found to represent transcripts lacking exons 4–7, 4–8, 4–6, or 5–8. *Lanes 10–12* contained RT-PCR products from RNA from normal lung tissues.

Fhit Protein Expression. Three independently prepared polyclonal rabbit anti-Fhit sera did not detect murine or rat Fhit protein in rodent tissues. Thus, purified human Fhit protein was injected into a chicken, and after the fourth injection, the antiserum was used in immunohistochemical analysis of several mouse tissues. Epithelial cells of various tissues expressed cytoplasmic Fhit, as shown in Fig. 6*A* for kidney reacted with a 1:600 dilution of the anti-Fhit serum; note the brown chromagen over the tubular epithelial cells. This pattern of staining matches that found for human kidney sections using anti-Fhit antiserum. Fig. 6*B* illustrates the specificity of the antibody detection; for this kidney section, purified gstFhit (not the immunogen, which was purified untagged Fhit) was included in the incubation of antiserum with tissue and has outcompeted the staining of the kidney tubule epithelia.

DISCUSSION

Cytogenetic studies had previously suggested the presence of a tumor or metastasis suppressor in the centromere proximal region of murine chromosome 14 (24). We became interested in this region when we previously mapped the murine *Ptprg* gene to centromere proximal chromosome 14 and characterized the intragenic homozygous deletion of *Ptprg* exons 3–5 in all cell clones derived from the original L cell strain, a cell strain established from adult male connective and adipose tissue after *in vitro* MCA treatment. Murine

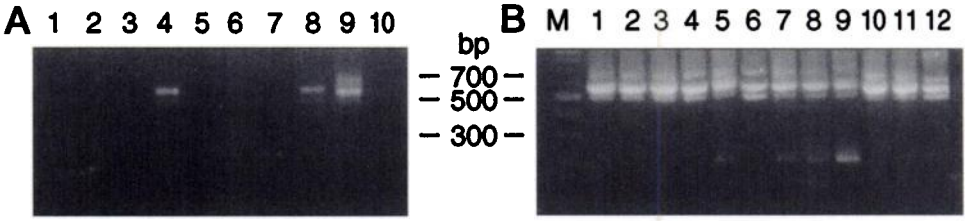

Fig. 5. Assessment of *Fhit* expression by RT-PCR analysis. *A*, murine cell or tissue RNA was reverse-transcribed, and single-stranded cDNA products served as templates for first-round PCR amplification with primers MF68F and MF843R to amplify exons 1–10; second-round amplification of exons 2–9 was with primers MF106F/MF792R. PCR products from mouse cell lines IT22 (*Lane 1*), CRL1412 (*Lane 2*), K1735M2X21 (*Lane 3*), ME2 (*Lane 4*), WEHI164 (*Lane 5*), LMTK$^-$ (*Lane 6*), K1735c110 (*Lane 7*), ME1 (*Lane 8*), adult mouse brain (*Lane 9*), and no cDNA template as negative control (*Lane 10*) were electrophoresed and visualized after ethidium bromide staining. *B*, murine lung tumor RNAs (*Lanes 1–9*) and normal lung RNAs (*Lanes 10–12*) were similarly reverse-transcribed followed by PCR amplification using primer pairs MF105F/MF826R and MF127F/MF806R for first- and second-round amplification.

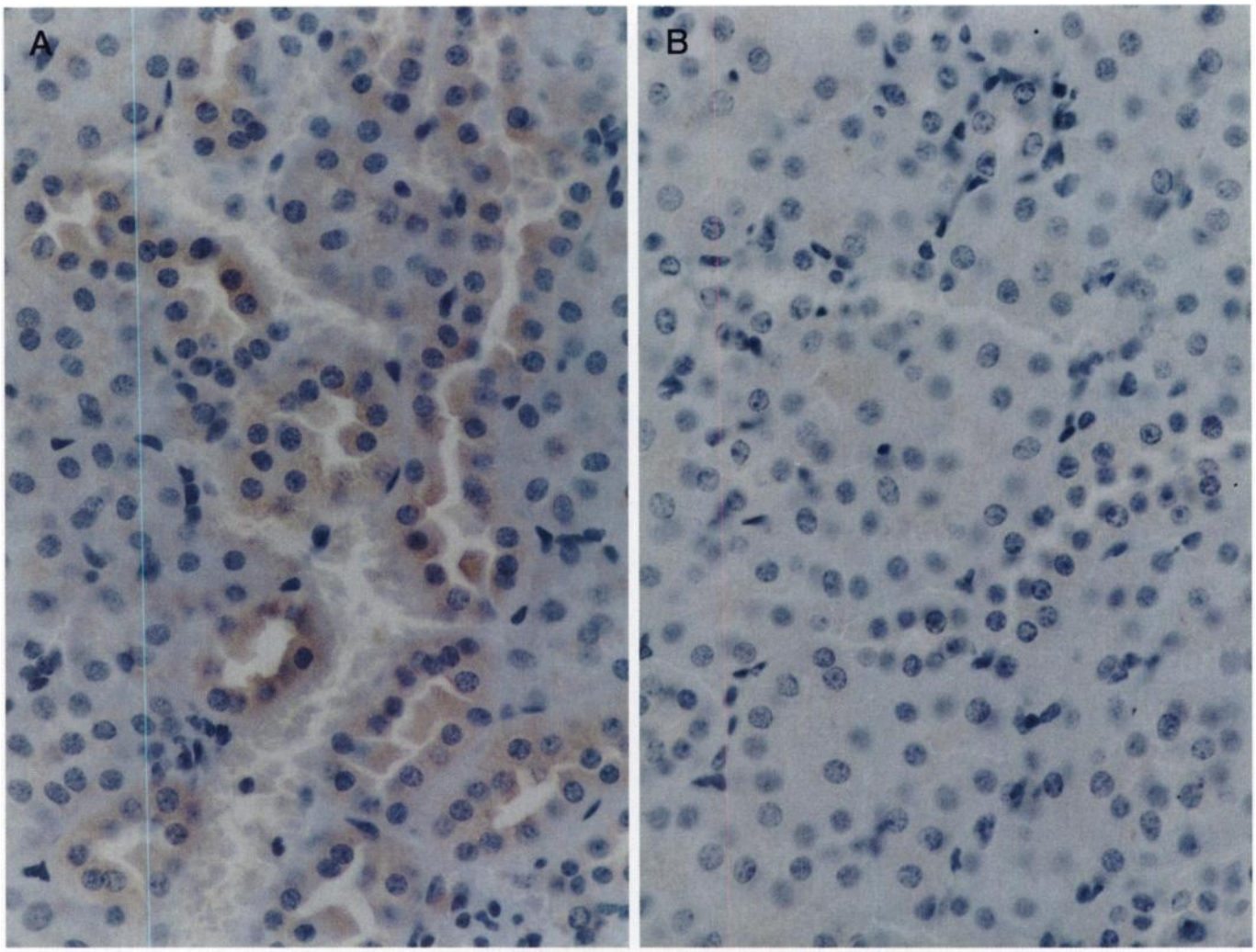

Fig. 6. Immunohistochemical analysis of *Fhit* expression in adult mouse tissues. Expression of endogenous Fhit in murine tissues was detected by immunohistochemical analysis using polyclonal chicken antiserum raised against purified human Fhit protein. Expression of Fhit was detected in adult mouse liver, esophagus, lung, and kidney paraffin sections as shown in *A* for kidney. The Fhit expression is detected as a brown stain in the cytoplasm confined to the tubular epithelium. *B*, a similar section from the same kidney, but purified gstFhit protein was added during the incubation with antiserum. Note that the gstFhit protein competed out the antibody staining. Sections were lightly counterstained with hematoxylin.

chromosome 14 is involved in t(14;14) translocations in the K-1735 parental melanoma, a murine lymphoma, a colon cancer cell line, and a mammary tumor (24).

The human *PTPRG* locus, encoding the PTPγ receptor tyrosine phosphatase gene, maps to human chromosome region 3p14.2 centromeric to a kidney cancer associated translocation break and the most inducible common human fragile site, *FRA3B* (28). The human *FHIT* gene crosses the same translocation break with its 5′ end and three untranslated exons on the centromeric side of the break, facing the 5′ end of the *PTPγ* gene. The *FRA3B* site is actually a broad region of fragility extending over the entire *FHIT* locus, with most fragile gaps induced by aphidicolin mapping from *FHIT* mid-intron 4 to mid-intron 5, flanking the first protein coding exon 5 (29). The human chromosome region 3p14.2 is involved in frequent allelic deletions, specifically within the *FHIT* gene, in most types of human cancer, perhaps because of breakage and repair of fragile breaks. We have cloned the murine homologue of the human *FHIT/FRA3B* region with several goals, the most important of which were to obtain clones for preparation of *Fhit* knockout mice, to determine whether the murine *Fhit* gene might also be altered in cancer cells, and to investigate the possible fragility of this locus in mice. In a parallel study, Glover *et al.* (30) have demonstrated that the mouse *Fhit* gene does, indeed, encompass a common fragile site.

The murine *Fhit* locus resembles the human homologue in its large size and position near the *Ptpγ* gene. The introns are large, and the portions of the locus sequenced are very low in GC content, like the human locus. The murine *Fhit* cDNA is highly homologous to the human cDNA, with an important difference. The murine cDNA has an open reading frame extending from exon 3 to exon 9, whereas the human open reading frame extends from exon 5 to exon 9; that is, in the human cDNA there is an in-frame stop codon upstream of the exon 5 starting Met codon, whereas in mouse *Fhit*, there is not an in-frame stop codon upstream of the analogous exon 5 Met within exon 5. Nevertheless, murine tissues most likely encode a protein starting with the exon 5 Met because the major transcript detected in all murine tissues and cell lines was a transcript lacking exon 3. A minor transcript, representing fewer than 10% of the cloned RT-PCR products, retains exons 3 and 4, but whether this transcript actually encodes a larger protein is not yet known.

In distribution and quantity, the expression pattern of *Fhit* mRNA in mouse adult tissues was very similar to that of human, as was protein expression in the tissues examined by immunohistochemistry or Western blot.

Expression of *Fhit* in murine cell lines, on the other hand, was unexpectedly low. It was difficult to detect *Fhit* expression in cell lines, even by RT-PCR and some cell lines, such as ME1 and ME2,

expressed an extremely low level of *Fhit* mRNA on Northern analysis, although the RT-PCR amplification showed expression of the expected products. Only one murine cell line, LMTK$^-$, expressed detectable levels of *Fhit* mRNA, and this mRNA was not of the normal size. LMTK$^-$ *Fhit* mRNA is aberrant, lacking exons 1–4 and instead containing a short sequence (~100 bp) of unknown origin at its 5′ end. It is possible that this transcript results from a rearrangement in intron 4, such as an insertion or translocation. Interestingly, this cell line carries a homozygous deletion within the nearby 5′ end of the *Ptpγ* gene (21). IT22TK$^-$ cells, derived from Swiss 3T3 cells after mutagenization and selection in 5-bromodeoxyuridine, also expressed an aberrant *Fhit* transcript, detected by hybridization to *Fhit* exons 1–4 but not by exons 5–10. MEL cells and RENCA cells, two cancer cell lines, do not express *Fhit* mRNA and exhibit homozygous deletions of exons 6–8 and exon 5, respectively. Thus, 4 of 11 transformed or malignant murine cell lines (not including ES, ME1, and ME2 cell lines) showed clear abnormalities of the *Fhit* locus. The abnormality in the IT22 cell line, a 3T3-derived clone, was unexpected, as was the very low level of expression of *Fhit* in F9 and ME cells, in which we have not detected *Fhit* protein by Western blot. It may be that embryonic and fetal cells express very low levels of *Fhit*, so that absence or low level *Fhit* expression in embryo-derived cell lines may be the expected result. This possibility is under investigation. Expression of *Fhit* mRNA and protein in tissues is very similar to expression in human tissues. Expression of *Fhit* RNA is lung tissue was easily detected by single-round RT-PCR, suggesting relatively abundant expression of *Fhit* in adult murine lung and possibly altered expression in a large fraction of lung tumors. In future experiments, reduction of expression of *Fhit* will be assessed by immunohistochemical analysis in murine lung tumors; absence of expression of *Fhit* in a large fraction of lung cancers would be consistent with involvement of *Fhit* alterations in murine lung carcinogenesis, as was previously suggested for human lung cancers (6, 13).

Our investigation of the murine *Fhit* locus, together with the demonstration of fragility of the mouse *Fhit* gene (30), suggests that the mouse will be an excellent model system to study the relationship between carcinogen treatment and alterations within the *Fhit* gene. Ultimately, the mouse model could also allow delineation of the relationship between *Fhit* alteration and tumor progression.

ACKNOWLEDGMENTS

We thank A. Mathis for preparation of the manuscript, Becky Cusick and Jean Letofsky for technical assistance, and Dr. Larry Barnes for helpful discussion and for purified human Fhit protein.

REFERENCES

1. Ohta, M., Inoue, H., Cotticelli, M. G., Kastury, K., Baffa, R., Palazzo, J., Siprashvili, Z., Mori, M., McCue, P., Druck, T., Croce, C. M., and Huebner, K. The *FHIT* gene, spanning the chromosome 3p14.2 fragile site and renal carcinoma-associated t(3;8) breakpoint, is abnormal in digestive tract cancers. Cell, *84:* 587–597, 1996.
2. Druck, T., Hadaczek, P., Fu, T-B., Ohta, M., Siprashvili, Z., Baffa, R., Negrini, M., Kastury, K., Veronese, M. L., Rosen, D., Rothstein, J., McCue, P., Cotticelli, M. G., Inoue, H., Croce, C. M., and Huebner, K. Structure and expression of the human *FHIT* gene in normal and tumor cells. Cancer Res., *57:* 504–512, 1997.
3. Inoue, H., Ishii, H., Alder, H., Snyder, E., Druck, T., Huebner, K., and Croce, C. M. Sequence of the *FRA3B* common fragile region: implications for the mechanism of *FHIT* deletion. Proc. Natl. Acad. Sci. USA, *94:* 14584–14589, 1997.
4. Virgilio, L., Schuster, M., Gollin, S. M., Veronese, M. L., Ohta, M., Huebner, K., and Croce, C. M. *FHIT* gene alterations in head and neck squamous cell carcinomas. Proc. Natl. Acad. Sci. USA, *93:* 9770–9775, 1996.
5. Michael, D., Beer, D. G., Wilke, C. W., Miller, D. E., and Glover, T. W. Frequent deletions of *FHIT* and *FRA3B* in Barrett's metaplasia and esophageal adenocarcinomas. Oncogene, *15:* 1553–1559, 1997.
6. Sozzi, G., Veronese, M. L., Negrini, M., Baffa, R., Cotticelli, M. G., Inoue, H., Tornielli, S., Pilotti, S., DeGregorio, L., Pastorino, V., Pierotti, M. A., Ohta, M., Huebner, K., and Croce, C. M. The *FHIT* gene at 3p14.2 is abnormal in lung cancer. Cell, *85:* 17–26, 1996.
7. Greenspan, D. L., Connolly, D. C., Wu, R., Lei, R. Y., Vogelstein, J. T. C., Kim, Y-T., Mok, J. E., Munoz, N., Bosch, X., Shah, K., and Cho, K. R. Loss of *FHIT* expression in cervical carcinoma cell lines and primary tumors. Cancer Res., *57:* 4692–4698, 1997.
8. Gemma, A., Hagiwara, K., Ke, Y., Burke, L. M., Khan, M. A., Nagashima, M., Bennett, W. P., and Harris, C. C. *FHIT* mutations in human primary gastric cancer. Cancer Res., *57:* 1435–1437, 1997.
9. Panagopoulos, I., Thelin, S., Mertens, F., Mitelman, F., and Aman, P. Variable *FHIT* transcripts in non-neoplastic tissues. Genes Chromosomes Cancer, *19:* 215–219, 1997.
10. van den Berg, A., Draaijers, T. G., Kok, K., Timmer, T., Van der Veen, A. Y., Veldhuis, P. M. J. F., de Leij, L., Gerhartz, C. D., Naylor, S. L., Smith, D. I., and Buys, C. H. C. M. Normal *FHIT* transcripts in renal cell cancer- and lung cancer-derived cell lines, including a cell line with a homozygous deletion in the *FRA3B* region. Genes Chromosomes Cancer, *19:* 220–227, 1997.
11. Siprashvili, Z., Sozzi, G., Barnes, L. D., McCue, P., Robinson, A. K., Eryomin, V., Sard, L., Tagliabue, E., Greco, A., Fusetti, L., Schwartz, G., Pierotti, M. A., Croce, C. M., and Huebner, K. Replacement of Fhit in cancer cells suppresses tumorigenicity. Proc. Natl. Acad. Sci. USA, *94:* 13771–13776, 1997.
12. Otterson, G. A., Xiao, G-H., Geradts, J., Jin, F., Chen, W., Niklinska, W., Kaye, F. J., and Yeung, R. S. Protein expression and functional analysis of the *FHIT* gene in human tumor cells. J. Natl. Cancer Inst. (Bethesda), *90:* 426–432, 1998.
13. Sozzi, G., Tornielli, S., Tagliabue, E., Sard, L., Pezzella, F., Pastorino, U., Minoletti, F., Pilotti, S., Ratcliffe, C., Veronese, M. L., Goldstraw, P., Huebner, K., Croce, C. M., and Pierotti, M. A. Absence of Fhit protein in primary lung tumors and cell lines with *FHIT* gene abnormalities. Cancer Res., *57:* 5207–5212, 1997.
14. Xiao, G-H., Jin, F., Klein-Szanto, A. J. P., Goodrow, T. L., Linehan, M. W., and Yeung, R. S. The *FHIT* gene product is highly expressed in the cytoplasm of renal tubular epithelium and is down-regulated in kidney cancers. Am. J. Pathol., *151:* 1541–1547, 1997.
15. Mao, L., Lee, J. S., Kurie, J. M., Fan, Y. H., Lippman, S. M., Lee, J. J., Ro, J. Y., Broxson, A., Yu, R., Morice, R. C., Kemp, B. L., Khuri, F. R., Walsh, G. L., Hittelman, W. N., and Hong, W. K. Clonal genetic alterations in the lungs of current and former smokers. J. Natl. Cancer Inst. (Bethesda), *89:* 857–862, 1997.
16. Wistuba, I. I., Lam, S., Behrens, C., Virmani, A. K., Fong, K. M., LeRiche, J., Samet, J. M., Srivastava, S., Minna, J. D., and Gazdar, A. F. Molecular damage in the bronchial epithelium of current and former smokers. J. Natl. Cancer Inst. (Bethesda), *89:* 1366–1373, 1997.
17. Yunis, J. J., and Soreng, A. L. Constitutive fragile sites and cancers. Science (Washington DC), *226:* 1199–1204, 1984.
18. Mao, L. Tumor suppressor genes: does *FHIT* fit? J. Natl. Cancer Inst. (Bethesda), *90:* 412–414, 1998.
19. Sambrook, J., Fritsch, E. F., and Maniatis, T. Molecular Cloning: A Laboratory Manual, Ed. 2. Cold Spring Harbor, NY: Cold Spring Harbor Laboratory, 1989.
20. Marini, J. C., Nelson, K. K., Battey, J., and Siracusa, L. D. The pituitary hormones arginine vasopressin-neurophysin II and oxytocin-neurophysin I show close linkage with interleukin-1 on mouse chromosome 2. Genomics, *15:* 200–202, 1993.
21. Wary, K., Lou, Z., Buchberg, A., Siracusa, L., Druck, T., LaForgia, S., and Huebner, K. A homozygous deletion in the carbonic anhydrase-like domain of the *Ptpg* gene in murine L cells. Cancer Res., *53:* 1498–1502, 1993.
22. Canzian, F., Gariboldi, M., Manenti, G., De Gregorio, L., Osada, S., Ohno, S., Dragani, T. A., and Pierotti, M. A. Expression in lung tumors and genetic mapping of the murine protein kinase Cn (nPKCn). Mol. Carcinog., *9:* 111–113, 1994.
23. Dragani, T. A., Falvella, F. S., Manenti, G., Pierotti, M. A., and Gambetta, R. A. Downexpression of aldehyde dehydrogenase 1 in murine lung tumors. Mol. Carcinog., *16:* 123–125, 1996.
24. Pathak, S., Dave, B. J., and Gadhia, P. K. Mouse chromosome 14 is altered in different metastatic murine neoplasias. Cancer Genet. Cytogenet., *83:* 172–173, 1995.
25. Williams, R. F., Pekarsky, Y., Cheng, S., and Gardiner, K. YAC clones targeting gene-rich regions of human chromosome 3. Mamm. Genome, *5:* 380–383, 1994.
26. Dragani, T. A., Manenti, G., and Della Porta, G. Quantitative analysis of genetic susceptibility to liver and lung carcinogenesis in mice. Cancer Res., *51:* 6299–6303, 1991.
27. Gariboldi, M., Manenti, G., Canzian, F., Falvella, F. S., Radice, M. T., Pierotti, M. A., Della Porta, G., Binelli, G., and Dragani, T. A. A major susceptibility locus to murine lung carcinogenesis maps on chromosome 6. Nat. Genet. *3:* 132–136, 1993.
28. Kastury, K., Ohta, M., Lasota, J., Moir, D., Dorman, T., LaForgia, S., Druck, T., and Huebner, K. Structure of the human receptor tyrosine phosphatase gamma gene (PTPRG) and relation to the familial RCC t(3;8) chromosome translocation. Genomics *32:* 225–235, 1996.
29. Zimonjic, D. B., Druck, T., Ohta, M., Kastury, K., Popescu, N. C., and Huebner, K. Positions of chromosome 3p14.2 fragile sites (*FRA3B*) within the *FHIT* gene. Cancer Res. *57:* 1166–1170, 1997.
30. Glover, T. W., Hoge, A., Miller, D. E., Askara-Wilke, J., Wilke, C. M., Adam, A., Dagenais, S. L., Dierick, H. A., and Beer, D. G. The murine *FHIT* gene is highly similar to its human orthologue and maps to a common fragile site region. Cancer Res., *58:* 3409–3414, 1998.